

A Protein Kinase Associated with Apoptosis and Tumor Suppression

STRUCTURE, ACTIVITY, AND DISCOVERY OF PEPTIDE SUBSTRATES*

Received for publication, May 10, 2001, and in revised form, June 28, 2001
Published, JBC Papers in Press, August 1, 2001, DOI 10.1074/jbc.M104273200

Anastasia V. Velentza^{‡§}, Andrew M. Schumacher^{‡¶}, Curtis Weiss[‡], Martin Egli^{||},
and D. Martin Watterson^{‡**}

From the [‡]Drug Discovery Program and Department of Molecular Pharmacology and Biological Chemistry, Northwestern University, Chicago, Illinois 60611 and the ^{||}Department of Biological Sciences, Vanderbilt University, Nashville, Tennessee 37235

Death-associated protein kinase (DAPK) has been implicated in apoptosis and tumor suppression, depending on cellular conditions, and associated with mechanisms of disease. However, DAPK has not been characterized as an enzyme due to the lack of protein or peptide substrates. Therefore, we determined the structure of DAPK catalytic domain, used a homology model of docked peptide substrate, and synthesized positional scanning substrate libraries in order to discover peptide substrates with K_m values in the desired 10 μ M range and to obtain knowledge about the preferences of DAPK for phosphorylation site sequences. Mutagenesis of DAPK catalytic domain at amino acids conserved among protein kinases or unique to DAPK provided a link between structure and activity. An enzyme assay for DAPK was developed and used to measure activity in adult brain and monitor protein purification based on the physical and chemical properties of the open reading frame of the DAPK cDNA. The results allow insight into substrate preferences and regulation of DAPK, provide a foundation for proteomic investigations and inhibitor discovery, and demonstrate the utility of the experimental approach, which can be extended potentially to kinase open reading frames identified by genome sequencing projects or functional genetics screens and lacking a known substrate.

mains include ankyrin repeats, P-loops, cytoskeleton binding motifs, a death domain, and a catalytic domain that has high sequence similarity to vertebrate myosin light chain kinase (MLCK). The protein kinase and death domains of DAPK have been directly implicated in cellular functions through the use of cultured cells transfected with DNA constructs encoding DAPK or mutated DAPK (1–3, 5). Although an intact kinase domain is required for many of these cellular functions, endogenous protein substrates for DAPK have yet to be identified, and an efficient peptide or protein substrate for the characterization of enzyme activity or development of inhibitors is not available.

The lack of known substrates for DAPK is reflective of an important challenge in the post-genomic sequence era (12). Complete genome sequences provide open reading frames (ORFs) that encode potential PKs, and functional genetics screens allow correlations of PKs with cell function with only a limited knowledge of downstream pathway components or enzyme mechanism. Characterization of the catalytic properties of the newly discovered PKs, linkage of quantitative changes in their enzyme activity to cellular responses, and discovery of ligands capable of modulating enzyme activity require the discovery of both peptide and protein substrates. These enzymes without known substrates are molecular orphans, and the rather strict substrate requirements of some can be an impediment to further research. DAPK is one such PK that has resisted identification of endogenous protein targets or useful peptide substrates with standard approaches (13). In turn, the lack of established DAPK protein substrates or an efficient peptide substrate has precluded the investigation of DAPK as an enzyme, impaired mechanistic investigations into the role of this interesting family of protein kinases in cell function, and hindered the search for selective inhibitors of DAPK. Quantitative phosphorylation of substrates is required for the analysis of the catalytic properties of DAPK, such as kinetic constants and substrate sequence preferences, and for investigations that require the determination of changes in enzyme activity. This is especially true when such activity changes occur without a corresponding change in the protein levels of the enzyme, as is often the case with intracellular signal transduction pathways (14). Therefore, a void exists in our knowledge about the catalytic and substrate recognition properties of DAPK and related death-associated PKs, and future research is impeded by the lack of this critical knowledge and key research tools. As part of an attempt to fill this void and provide a proof of principle for an integrated approach to kinase substrate discovery, we investigated DAPK using an approach that includes the interface of very high resolution macromolecular crystallography and positional scanning substrate library synthesis linked to enzymology.

We report the discovery of useful peptide substrates for

Death-associated protein kinase (DAPK)¹ is a multidomain, calmodulin (CaM)-regulated serine/threonine protein kinase (PK) that has been implicated in apoptosis (1–5), tumor suppression (5), susceptibility to human disease (6–10), and ischemia-induced neuronal cell death (11). DAPK's multiple do-

* This work was supported in part by grants from the Alzheimer's Association, the Institute for the Study of Aging, and by Grants T32-AG00260 and S10-RR13810 from the National Institutes of Health. The costs of publication of this article were defrayed in part by the payment of page charges. This article must therefore be hereby marked "advertisement" in accordance with 18 U.S.C. Section 1734 solely to indicate this fact.

§ Postdoctoral scholar of the Drug Discovery Program.

¶ Predoctoral scholar of the Drug Discovery Program.

** John G. Searle Professor of Molecular Biology and Biochemistry. To whom correspondence should be addressed: Northwestern University, 303 E. Chicago Ave. Ward 8-196, Chicago, IL 60611. Tel.: 312-503-0656; Fax: 312-503-1300; E-mail: m-watterson@northwestern.edu.

¹ The abbreviations used are: DAPK, death-associated protein kinase; ORFs, open reading frame; MALDI-TOF MS, matrix-assisted laser-desorption mass spectrometry; CaM, calmodulin; CAMK, CaM kinase; CaMKK, CaMK kinase; MLCK, myosin light chain kinase; PK, protein kinase; PAGE, polyacrylamide gel electrophoresis; r.m.s., root mean square; PHK, phosphorylase kinase; PDB, protein data bank; AMPNP, adenosine 5'-(β , γ -imino)triphosphate.

DAPK that allows characterization of its catalytic properties. The final substrates have K_m values in the target range of 10 μM , which is needed for the measurement of a kinase activity in biological samples. This allowed us to monitor DAPK catalytic activity in extracts of adult brain and to measure an enrichment in specific activity that correlated with protein purification detected by Western blot analysis with antisera against the catalytic domain. The insight into phosphorylation site preferences emanating from knowledge of catalytic domain activity and structure should be useful in future searches for endogenous protein substrates and the development of selective inhibitors. The results also provide a proof of principle for an approach that can potentially be applied to any ORF encoding a protein kinase.

EXPERIMENTAL PROCEDURES

Enzyme Production, Purification, and Assay—The DAPK catalytic domain was produced by polymerase chain reaction-assisted subcloning (15) from the DAPK cDNA, kindly provided by A. Kimchi (1), using the primers 5'-GGG GGG GGT CTC AGC GCT CTT GAT CCA GGG ATG CTG CAA-3' and 5'-GGG GGG GGT CTC AGC GCT ACT AAG TGC CTG TTG TGT ATC-3', which contained flanking *Bsa*I sites and amplified the portion of the cDNA from nucleotides 337–1191 (GenBank™ accession number NM_004938). Briefly, the region of the DAPK cDNA that encodes amino acids 1–274, corresponding to the similar catalytic region produced from MLCK (16), was subcloned into the pASK-IBA3 (Sigma) expression vector at the *Bsa*I sites. Protein was produced and purified from *Escherichia coli* essentially as described previously (16) except with the additional use of the streptavidin tag following the manufacturer's recommendations. The protein was homogeneous by SDS-PAGE and gave the expected molecular weight.

DAPK was enriched from bovine brain extracts using a modification of the first few steps of MLCK purification (16), with all purification steps carried out at 4 °C. Briefly, bovine brain was homogenized in 2 volumes of buffer A (20 mM Tris-HCl, pH 7.3, 1 mM EDTA, 1 mM dithiothreitol, 1 mg/liter pepstatin and leupeptin, 40 mM 1-chloro-3-tosylamido-7-amino-2-heptanone) in a Waring blender at low speed, centrifuged at 10,000 $\times g$ for 30 min in a Sorvall SLA-3000 rotor, and the supernatant subjected to a 55% saturated ammonium sulfate precipitation. The 55% ammonium sulfate pellet was resuspended in 1 volume of buffer B (20 mM Tris, pH 8.0, 1 mM EDTA, and 1 mM dithiothreitol), and its conductivity was adjusted to that of buffer B. The redissolved fraction was adsorbed to a DEAE-cellulose column equilibrated with buffer B, washed with 5 column volumes of buffer B, and DAPK eluted with buffer B containing 0.2 M NaCl. All chromatography fractions were assayed immediately for DAPK enzyme activity using peptide 38 described in this report, and aliquots were prepared in SDS-PAGE sample buffer for subsequent Western blot analysis. Western blot analyses were done as described (17) with a site-directed polyclonal rabbit antisera (number 7315) made against the synthetic peptide KPKDTQQALSRLK using a protocol described previously for antibody production (18). This amino acid sequence corresponds to a region of the DAPK ORF that encodes the proposed catalytic domain.

Enzyme assays and kinetic analyses were done essentially as described previously (16–18) for MLCK and MLCK catalytic domain protein but using the DAPK catalytic domain protein made in *E. coli* or DAPK purified from bovine brain. Peptide substrate phosphorylation by DAPK was linear under the conditions used, and less than 10% of the peptide was consumed in each reaction. Kinetic data were analyzed by double-reciprocal (Lineweaver-Burk) plots using Prism version 2.0 (GraphPad Software Inc.). Autophosphorylation of endogenous DAPK was examined *in vitro* as described previously for calmodulin-dependent protein kinase II (19). Briefly, enriched fractions from the DEAE-cellulose chromatography purification step of endogenous DAPK from bovine brain (described here), or commercially available calmodulin-dependent protein kinase II as a control, were incubated for 10 min at 25 °C in the presence of [γ - ^{32}P]ATP. The reaction was terminated by addition of SDS-containing sample buffer, and samples were subjected to SDS-PAGE. ^{32}P -Labeled proteins were visualized by STORM PhosphorImager (Molecular Dynamics) after 1 and 14 h of exposure.

Peptide Synthesis—Peptide synthesis was done by solid phase synthesis, as described previously (20), using a parallel synthesis of each peptide, except that the guanyl group of Arg was protected with 2,2,4,6,7-pentamethylidihydrobenzofuran-5-sulfonyl, and 30 mg of Rink-amide resin (0.8 mmol of nitrogen/g) from Advanced ChemTech

(Louisville, KY) was used. Peptides were cleaved from the resin by treatment for 3 h using a mixture of trifluoroacetic acid/anisole/dithioethanol (90:5:5 v/v/v) at room temperature. Peptides were precipitated with ethyl ether, washed, and extracted with 5% (v/v) acetic acid, lyophilized, and then purified by reverse phase-high pressure liquid chromatography on a preparative Chromosorb (Rainin Instruments, Woburn, MA) C18 column using gradients of 0.1% (v/v) trifluoroacetic acid in water and 60% aqueous acetonitrile containing 0.08% trifluoroacetic acid. Purified peptides were characterized by matrix-assisted laser-desorption mass spectrometry (MALDI-TOF MS) using a Perspectives (Foster City, CA) Voyager DE-Pro system and by amino acid composition analysis of acid hydrolysates on a Waters (Bedford, MA) Alliance 2690 separations system equipped with a Waters 996 photo-diode array detector as described previously (20).

DAPK Structure and Peptide Substrate Homology Model—The DAPK catalytic domain structure was determined to a resolution of 1.5 Å, and structural information was deposited with the protein data bank (PDB) as file 1IG1. Details of crystallographic data collections and statistics of refinement for the DAPK catalytic domain alone (apoI and apoII), the binary complex with the ATP analog, AMPPNP, and the ternary complexes with AMPPNP/Mg $^{2+}$ or AMPPNP/Mn $^{2+}$ will be presented elsewhere.² For the purpose of peptide substrate discovery research reported here, orthorhombic crystals were grown from gradients of ammonium sulfate by the hanging-drop vapor diffusion method, and diffraction data were collected at the Advanced Photon Source, Argonne, IL. Crystals used for data collection contained one protein molecule per crystallographic asymmetric unit and diffracted to 1.5 Å. The structure of the high resolution orthorhombic crystals was determined by the single wavelength anomalous diffraction technique and used methyl mercury chloride soaks. Orthorhombic crystals of the binary complex with AMPPNP were obtained by co-crystallization, and orthorhombic crystals of the ternary complex were obtained by soaks of the binary complex crystals in metal ion solutions. The structures of ternary complexes in the presence of Mg $^{2+}$ and Mn $^{2+}$ ions were found similarly. The r.m.s. deviation between apoI and binary complex is 0.68 Å. The r.m.s. deviations between apoI and the ternary complexes do not exceed 0.7 Å.

For homology modeling of a bound peptide substrate docked into the DAPK active site, the structure for the phosphorylase kinase (PHK) heptapeptide substrate RQMSFRL bound in the active site of the phosphorylase kinase catalytic domain was obtained from the protein data bank (code 2PHK). The phosphorylase kinase structure was that determined previously by Lowe *et al.* (21) to a resolution of 2.6 Å. The Biopolymer and Homology modules of Insight II (MSI; San Diego, CA) were used to align and superimpose the DAPK catalytic domain and that of phosphorylase kinase and its bound substrate found in code 2PHK. The two catalytic domain amino acid sequences were aligned for maximum sequence similarity, and the two catalytic domain crystal structures were superimposed by use of automatic structural alignment within the Homology module. The r.m.s. of the superimposed structures was 0.9.

RESULTS

DAPK Catalytic Domain—As summarized in Fig. 1, the catalytic domain of DAPK has amino acid sequence similarity to the corresponding region of the MLCK catalytic domain (~44% identity) and the phosphorylase kinase catalytic domain (33% identity). However, a crystal structure of the MLCK catalytic domain is not available, whereas a high resolution crystal structure of phosphorylase kinase is available. In addition, phosphorylase kinase is one of the few serine/threonine PKs for which there is a three-dimensional structure of a kinase domain containing a bound peptide substrate (21). Therefore, the corresponding catalytic domain region of DAPK (Fig. 1) was made by polymerase chain reaction-based subcloning of the appropriate region of the cDNA into a protein expression vector, and protein made in *E. coli* was described under "Experimental Procedures." The protein was purified based on the predicted properties of the ORF for the catalytic domain and utilization of an expressed affinity tag at the carboxyl terminus. The catalytic domain and protein production in *E. coli*

² Tereshko, V., Teplova, M., Brunzelle, J., Watterson, D., and Egli, M. (2001) *Nature Struct. Biol.*, in press.

FIG. 1. Alignment of the amino acid sequences of the catalytic domains of death-associated protein kinase, phosphorylase kinase, and myosin light chain kinase. The amino acid sequence of the human DAPK catalytic domain (*huDAPK*) and the corresponding regions from human phosphorylase kinase (*huPHK*) and human myosin light chain kinase (*huMLCK*) are shown along with numbering and notations of selected amino acids in DAPK examined in this study. The threonine following the initiator methionine is taken as residue 1 for *huDAPK*. The amino acid sequences were aligned using the Clustal method in MegAlign (DNASTAR, Madison, WI). Features of DAPK addressed in the text are denoted with the following symbols: *, ATP site residues conserved among serine/threonine protein kinases; +, novel ATP site residue in DAPK and MLCK; **, conserved active site residues mutated in DAPK as part of this study; *I*, amino acids in close proximity to the substrate phosphorylation site sequence positions in the DAPK structural model and mutated in DAPK as part of this study; and —, basic charge loop in the DAPK catalytic domain structure, composed of an amino acid sequence conserved among death kinases and mutated in DAPK as part of this study.

<i>huDAPK</i>	T V F R Q E N V D D Y Y D T - - - G E E L G S G Q F A V V K	27
<i>huPHK</i>	P - - D S H S A Q D F Y E N Y E P K E I L G R G V S S V R	34
<i>huMLCK</i>	T I N T E Q K V S D F Y D I - - - E E R L L G S G K F G Q V F	1479
<i>huDAPK</i>	K C R E K S T G L Q Y A A K F I K - - - - K R R T K S S R	52
<i>huPHK</i>	R C I H K P T S Q E Y A V K V I D V T G G G S F S P E E V R	64
<i>huMLCK</i>	R L V E K K T R K V W A G K F F K - - - - A Y S A K E - -	1502
<i>huDAPK</i>	R G V S R E D I E R E V S I L K E I Q - H P N V I T L H E V	81
<i>huPHK</i>	E - - L R E A T L K E V D I L R K V S G H P N I I Q L K D T	92
<i>huMLCK</i>	- - - - K E N I R Q E I S I M N C L H - H P K L V Q C V D A	1527
<i>huDAPK</i>	Y E N K T D V I L I L E L V A G G E L F D F L A E K E - S L	110
<i>huPHK</i>	Y E T N T F F F L V F D L M K R G E L F D Y L T E K - V T L	121
<i>huMLCK</i>	F E E K A N I V M V L E I V S G G E L F E R I I D E D F E L	1557
<i>huDAPK</i>	T E E E A T E F L K Q I L N G V Y Y L H S L Q I A H F D L K	140
<i>huPHK</i>	S E K E T R K I M R A L L E V I C T L H K L N I V H R D L K	151
<i>huMLCK</i>	T E R E C I K Y M R Q I S E G V E Y I H K Q G I V H L D L K	1587
<i>huDAPK</i>	* * I M L L D R N V P K P R I K I I D F G L A H K I D F G	170
<i>huPHK</i>	P E N I L L D D N M - - - N I K L T D F G F S C Q L E P G	177
<i>huMLCK</i>	P E N I M C V N K T G T - - R I K L I D F G L A R R L E N A	1615
<i>huDAPK</i>	N E F K N I F G T P E F V A P E I V N Y - - - E P L G L -	195
<i>huPHK</i>	E R L R E V C G T P S Y L A P E I I E C S M N E D H P G Y G	207
<i>huMLCK</i>	G S L K V L F G T P E E F V A P E V I N Y - - - E P I G Y -	1640
<i>huDAPK</i>	- E A D M W S I G V I T Y I L L S G A S P F L G D T K Q E T	224
<i>huPHK</i>	K E V D M W S T G V I M Y T L L A G S P P F W H R K Q M L M	237
<i>huMLCK</i>	- A T D M W S I G V I C Y I L V S G L S P F M G K D N D N E T	1669
<i>huDAPK</i>	L A N V S A V N Y E F E D E Y F S N T S A L A K D F I R R L	254
<i>huPHK</i>	L R M I M S G N Y Q F G S P E W D D Y S D T V K D L V S R F	267
<i>huMLCK</i>	L A N V T S A T W D F D D E A F D E I S D D A K D F I S N L	1699
<i>huDAPK</i>	L V K D P K K R M T I Q D S L Q H P W I	274
<i>huPHK</i>	L V V Q P Q N R Y T A E E A L A H P P F	287
<i>huMLCK</i>	L K K D M K N R L D C T Q C L Q H P W L	1719

were used for structure determination by high resolution x-ray crystallography, peptide substrate discovery by positional scanning substrate library synthesis, kinetic analysis of DAPK catalytic properties, and probing of the linkage between DAPK structure and activity by site-directed mutagenesis. This provided the knowledge and tools required for subsequent comparative analysis of the enzyme properties of DAPK from vertebrate tissue.

In order to gain insight into structural features of DAPK, the high resolution (1.5 Å) crystal structure of DAPK was determined. The structure is available from the PDB as code 1IG1. The DAPK catalytic domain is in the active closed conformation (Fig. 2A) and is the highest resolution crystallographic structure available for a protein kinase. The phylogenetically conserved amino acid residues involved in protein kinase interactions with ATP substrate and the conserved lysine important for catalysis (indicated in Fig. 1) are found in the corresponding positions of the DAPK structure, which contains a standard non-hydrolyzable ATP analog in its structure. In addition to the various conserved features of serine/threonine protein kinases in the ATP substrate site, the high resolution structure of DAPK reveals several novel features. For example, there is a methionine (Met-145) in close proximity to the ATP analog in the DAPK structure. Leucine is a more common amino acid found at this position in other serine/threonine protein kinases for which crystal structures have been solved.

The DAPK structure also has novel features outside of the ATP recognition region. For example, a basic loop structure that includes a cluster of lysine and arginine residues in the sequence from Lys-44 to Val-55 (indicated in Fig. 1) is found in a region close to the potential peptide substrate recognition region of the catalytic domain, based on homology with other kinases. This basic loop is found only in the DAPK structure. However, the amino acid sequences of other serine/threonine protein kinases, such as Dlk (22), DRP-1 (4), DAPK2 (23), DRAKs (24), and ZIP kinase (25), have a similar cluster of basic amino acids. Because most of these enzymes have been implicated in regulation of cell death and DAPK is the first structure

available for this family of serine/threonine protein kinases, the possible importance of this basic loop structure in substrate recognition was addressed by site-directed mutagenesis after an efficient substrate was discovered (see below).

The remarkable similarity between the structure of DAPK determined as part of this investigation and that previously reported (21) for phosphorylase kinase containing a bound peptide substrate provided insight into what regions of DAPK are potentially important for recognition of a peptide substrate core phosphorylation sequence, composed of an RXXSX motif. Therefore, the DAPK catalytic domain (amino acids 1–274) and that of the corresponding region from phosphorylase kinase (amino acids 7–287) were aligned for maximum sequence similarity, and the two structures were superimposed with an excellent fit (r.m.s. 0.9) as described under “Experimental Procedures.” The excellent superimposition of the two catalytic domains allowed the use of the bound peptide substrate from the phosphorylase kinase structure as a model for DAPK peptide substrate discovery. The superimposed structures revealed that the phosphorylase kinase peptide substrate docks with the DAPK structure (Fig. 2B) such that discrete amino acids in DAPK in close proximity to the docked substrate can be compared with their corresponding amino acids in phosphorylase kinase (Table I and Fig. 1). Although peptide analogs of the phosphorylase kinase substrate do not serve as *in vitro* substrates for the DAPK catalytic domain, the comparison of common and unique residues in the two kinases can provide a focal point for initiation of peptide substrate discovery for DAPK.

Close inspection reveals that the amino acids from DAPK that are in close proximity to each position of the modeled peptide substrate are conserved compared with phosphorylase kinase, as is the spacing between these residues. For example, P-3 of the peptide substrate interacts with Glu-110, Phe-112, and Glu-153 of phosphorylase kinase, and the equivalent positions of DAPK are Glu-99, Phe-101, and Glu-142. Selected examples are given in Table I. These comparisons provide structural insight into the known preference for an arginine residue at P-3 and suggested that this position should be held

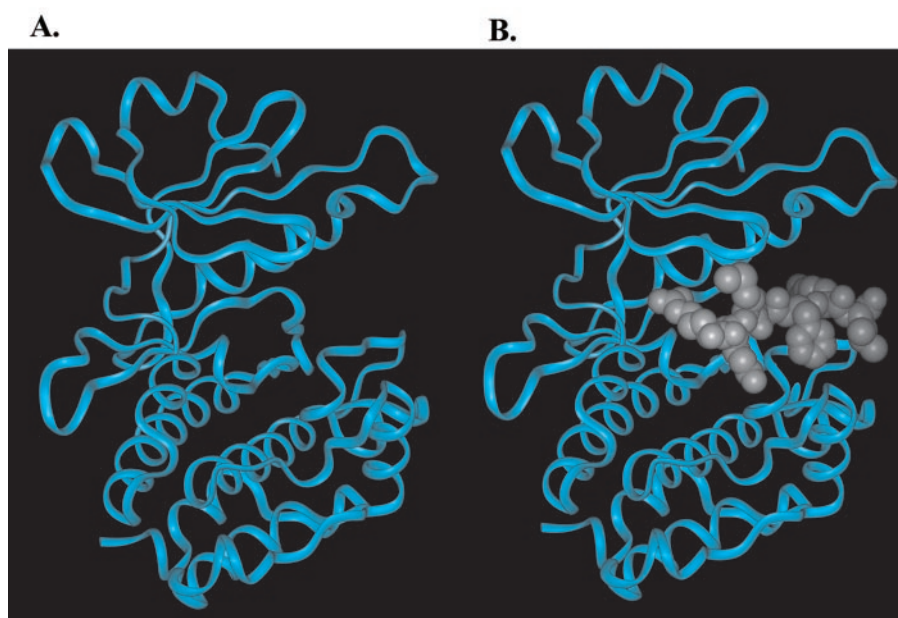


FIG. 2. Structure of the DAPK catalytic domain. The 1.5-Å crystal structure of the DAPK catalytic domain in the active closed conformation is shown in *A*, and the DAPK structure with a docked peptide substrate model is shown in *B*. The DAPK structure is that determined as part of this study and can be found as PDB code 11G1. The modeled peptide substrate is based on the bound substrate in the PDB code 2PHK, a crystal structure of a ternary complex determined by Lowe *et al.* (21). Docking of the modeled peptide into the DAPK structure by use of homology modeling is described in the text.

TABLE I

Amino acids in DAPK structure proximal to docked substrate

Proximal is defined as an average distance of 5 Å between amino acids of DAPK and β -carbon atoms of substrate amino acids. Substrate is the docked PHK substrate from PDB code 2PHK as described in the text.

Peptide substrate position	Amino acid in DAPK	Amino acid in PHK
P - 3	Glu-99	Glu-110
	Phe-101	Phe-112
	Glu-142	Glu-153
P - 2	Glu-181	Ser-188
	Lys-140	Lys-151
	Glu-142	Glu-153
	Phe-182	Tyr-189
P - 1	Ser-20	Arg-27
	Gly-21	Gly-28
	Gln-22	Val-29
	Lys-140	Lys-151
P0	Gln-22	Val-29
	Asp-138	Asp-149
	Lys-140	Lys-151
	Asp-160	Asp-167
	Leu-163	Phe-170
	Gly-178	Gly-185
P1	Thr-179	Thr-186
	Gln-22	Val-29
	Ile-176	Val-183
	Pro-180	Pro-187
	Gly-178	Gly-185
	Val-183	Leu-190

constant for initial positional scanning substrate library syntheses.

The docked model substrate is also consistent with established preference of serine/threonine protein kinases for a serine or threonine side chain *versus* a tyrosine side chain as the phospho-acceptor in the kinase reaction. For example, examination of this position of the homology model peptide substrate reveals that there is sufficient volume in the DAPK structure to accommodate a serine or threonine side chain but not a tyrosine side chain. Again, the structural comparisons provided insight into substrate preferences at this position and suggested that P0 should be held constant with a serine or threonine for initial positional scanning substrate library syntheses.

In contrast to the remarkable level of conservation of the DAPK structure around the P -3 and P0 interacting regions, key differences between DAPK and phosphorylase kinase are found at positions interacting with the core phosphorylation site of the docked substrate. For example, P -2 proximal amino acids of phosphorylase kinase are Ser-188, Tyr-189, and Gln-234, but residues at the corresponding positions of the DAPK structure are Glu-181, Phe-182, and Lys-221. Other examples, including structural conservations between the two kinases at these positions, are provided in Table I. Overall, the comparative analyses suggested that variations at substrate positions P -2, P -1, and P1 might be important points for discovery of useful substrates for DAPK and might provide a basis for selective substrate utilization among DAPK, phosphorylase kinase, MLCK, and other closely related kinases.

The DAPK structure also suggests features of substrates outside of the core phosphorylation site that should be considered. For example, upstream of the region of DAPK implicated by the docked peptide model in core phosphorylation sequence recognition, there are two clusters of acidic amino acids (Glu-112, Glu-113, Glu-114, Glu-117 and Glu-234, Glu-236, Glu-238) and a single acidic amino acid (Glu-106) that might contribute a charge complementarity to basic amino acids in a substrate sequence upstream of the substrate core phosphorylation site. In other words, basic amino acids in the P -6 through P -8 of a DAPK substrate might contribute to the substrate recognition features.

Overall, analysis of the DAPK structure suggests specific sets of amino acids in DAPK that are 1) conserved and potentially interact with the strictly conserved substrate positions P -3 and P0; 2) are variable and potentially contribute to interactions at positions P -2, P -1, and P1; and 3) are part of topological features of DAPK that may contribute to interactions with basic amino acids in the substrate that are upstream of the core phosphorylation site sequence. It is hypothesized that the combination of common and unique features are major contributors to the ability of DAPK to discriminate among closely related substrate sequences in the area around the phosphorylation site. This combination of structural comparisons and peptide substrate docking suggested a peptide substrate with the pattern of (R/K)(R/K)(R/K)XXRXXSX, where X is any amino acid and (R/K) could be either arginine or lysine at

TABLE II
Positional scanning substrate library peptides used in this study

Peptides were synthesized, purified, and characterized by high pressure liquid chromatography, composition analysis, and MALDI-TOF mass spectrometry as described under "Experimental Procedures."

Peptide	Sequence	Peptide	Sequence	Peptide	Sequence
1	KKRPQRATSNVF	25	KKRPQRRGSNVF	49	KKRPQRRYSPVF
2	KKRPQRRTSNVF	26	KKRPQRRHSNVF	50	KKRPQRRYSWVF
3	KKRPQRNTSNVF	27	KKRPQRRLSNVF	51	KKRPQRRYSYVF
4	KKRPQRDTSNVF	28	KKRPQRRISNVF	52	KKRPQRRYSVVF
5	KKRPQRQTSNVF	29	KKRPQRRKSNVF	53	KKRPQRRLSAVF
6	KKRPQRETSNVF	30	KKRPQRRMSNVF	54	KKRPQRRLSRVF
7	KKRPQRGTSNVF	31	KKRPQRRFSNVF	55	KKRPQRRLSNVF
8	KKRPQRHTSNVF	32	KKRPQRRPSNVF	56	KKRPQRRLSQVF
9	KKRPQRLLTSNVF	33	KKRPQRRWSNVF	57	KKRPQRRLSQVF
10	KKRPQRITSNVF	34	KKRPQRRYSNVF	58	KKRPQRRLSEVF
11	KKRPQRKTSNVF	35	KKRPQRRVSNVF	59	KKRPQRRLSGVF
12	KKRPQRMTSNVF	36	KKRPQRRYSAVF	60	KKRPQRRLSHVF
13	KKRPQRFTSNVF	37	KKRPQRRYSRVF	61	KKRPQRRLSLVF
14	KKRPQRPTSNVF	38	KKRPQRRYSQVF	62	KKRPQRRLSIVF
15	KKRPQRSTSNVF	39	KKRPQRRYSDFV	63	KKRPQRRLSKVF
16	KKRPQRWTSNVF	40	KKRPQRRYSQVF	64	KKRPQRRLSMVF
17	KKRPQRYSNVF	41	KKRPQRRYSEVF	65	KKRPQRRLSFVF
18	KKRPQRVTSNVF	42	KKRPQRRYSGVF	66	KKRPQRRLSPVF
19	KKRPQRRASNVF	43	KKRPQRRYSHVF	67	KKRPQRRLSWVF
20	KKRPQRRRSNVF	44	KKRPQRRYSLVF	68	KKRPQRRLSYVF
21	KKRPQRRNSNVF	45	KKRPQRRYSIVF	69	KKRPQRRLSVVF
22	KKRPQRRDSNVF	46	KKRPQRRYSKVF	70	KKRPQRRYTNVF
23	KKRPQRRQSNVF	47	KKRPQRRYSMVF	71	KKRPQRRYYNVF
24	KKRPQRRFSNVF	48	KKRPQRRYSFVF		

the noted position, as a starting point in positional scanning substrate library synthesis.

Positional Scanning Substrate Library Synthesis and Activity Screens—As noted above, the details of the DAPK structure and the docked peptide substrate model suggested the potential utility of synthesizing positional scanning substrate libraries for P -2, P -1, and P1 in the context of a peptide sequence of (R/K)(R/K)(R/K)XXRXXSX. Although the positional scanning substrate library approach had been used successfully with protease peptide substrate discovery (26), it has not been used in kinase substrate discovery. Therefore, we focused our initial proof of principal investigations on peptide discovery by variation of substrate positions P -2, P -1 and P1 based on the docked peptide substrate model.

The next decision was the choice of a starting peptide substrate sequence that would fit the suggested motif of (R/K)(R/K)(R/K)XXRXXSX and could be used initially to vary the four positions suggested by the structural model. A diverse array of potential sequences could be used. We made our choice based, again, on homology arguments. Specifically, MLCK has high sequence similarity with DAPK in the catalytic domain (Fig. 1) and has a preference for protein and peptide substrates with the motif noted above, as do a variety of serine/threonine protein kinases. Therefore, a peptide analog of the myosin light chain phosphorylation site, peptide 1 (KKRPQRATSNVF), was used as a starting point. Peptide 1 was a poor substrate for DAPK, and attempts to estimate a K_m indicated a value greater than 150 μM . Regardless, the production of phosphorylated product was sufficient to allow quantitative measurement in a screening assay (see "Experimental Procedures").

The primary goal of the positional scanning substrate library synthesis approach was the rapid discovery of peptide substrates with K_m values in the desired range of $\sim 10 \mu\text{M}$. Peptide substrates with K_m values in the 10 μM range allow the characterization of the enzymatic properties of a kinase and subsequent development of an enzyme assay for measurement of activity in biological samples. A secondary goal of the approach was the coincident discovery of peptide substrates with some selectivity for DAPK over closely related kinases. This enhances the potential for discovery of substrates useful in the

development of an assay for measurement of enzyme activity in biological samples. Optimization of the core phosphorylation site sequence is not the goal of the positional scanning substrate library synthesis approach. Although the approach can result in an insight into substrate preferences for an enzyme and some optimization is realized, there is a theoretical limit to how high an affinity a substrate can possess for an enzyme and still allow facile product release, and there is little evidence that evolved enzyme systems in nature use optimal substrates to bring about their biological effects. As described below, we obtained an improvement in activity greater than 10-fold through the manipulation of only three positions in the original substrate sequence, and later variations suggested that an optimal sequence was not obtained as part of these investigations.

Starting with peptide 1 (KKRPQRATSNVF), we used the recursive synthesis and activity screening of peptide substrate libraries inherent to the positional scanning approach. Specifically, we synthesized a library of peptides that varied from each other within the core phosphorylation sequence by a single amino acid at P -2, and we screened each purified peptide for its relative ability to serve as a substrate for DAPK. All peptides were also tested for their ability to serve as MLCK substrates in order to address selectivity for DAPK, since an MLCK peptide substrate was used as a starting sequence. An efficient peptide substrate from the P -2 library that is also selective for DAPK *versus* MLCK was used as the basis for selection of amino acids to hold constant at P -2, and a subsequent peptide substrate library was made that varied at the next position, P -1. The process was repeated for P1. Cysteine was avoided in each library for technical reasons, such as variable recovery due to disulfide formation or oxidation, and serine was excluded at positions other than P0 in order to avoid the complications of data interpretation in a high throughput analysis by introduction of a second phosphorylatable serine.

The peptides synthesized, purified, and characterized as part of this study are shown in Table II, and the relative activity data obtained during screening assays with DAPK are summarized in Fig. 3. Verification of synthesis was done by MALDI-TOF MS and composition analyses of the purified peptides.

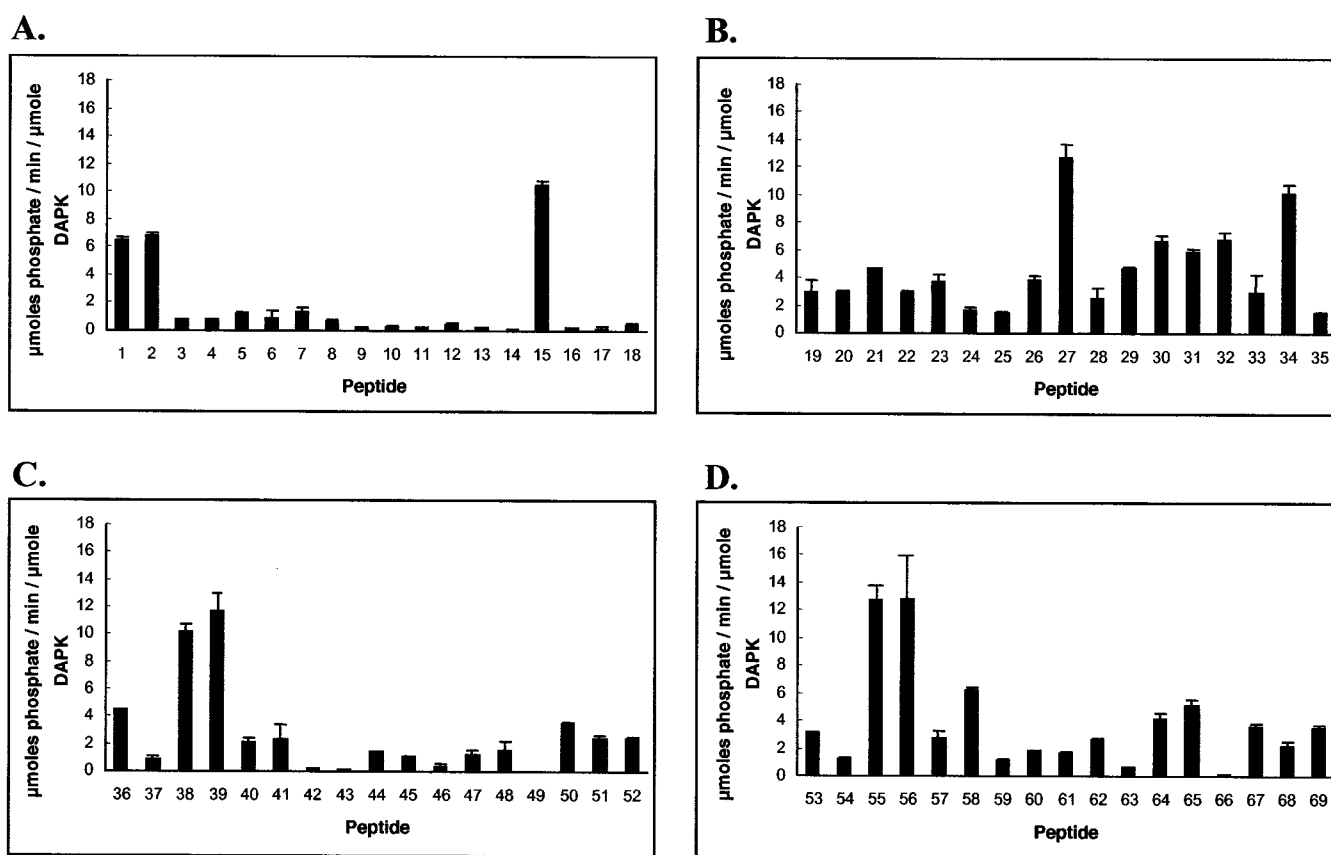


FIG. 3. **Activity screening of DAPK peptide substrate libraries.** The libraries synthesized as part of this study differed by variation of the starting peptide sequence KKRQRATSNVF at the P - 2 (A), P - 1 (B), P1 with Tyr at P - 1 (C), or P1 with Leu at P - 1 (D). The specific activity of DAPK (micromoles of phosphate incorporated into peptide substrate per μmol of DAPK per min) for each purified peptide substrate is shown. Peptide numbers correspond to the sequences given in Table II. Data represent the average \pm the range of values for duplicates.

This approach allowed the discovery of improved peptide substrates and provided insight into the relative substrate preferences of DAPK. The desirable peptide substrates discovered by the screen were then characterized further in terms of preference for phosphate acceptor side chain at P0 and, finally, used in kinetic analyses with DAPK.

The first library of 18 peptides had the amino acid sequence KKRQRXTSNVF, where *X* indicates the presence of one of the genetically encoded common amino acids. Peptides 1–18 were made in a parallel set of reactions, and each was purified to chemical homogeneity as determined by amino acid composition and mass spectrometry analysis. The purified and characterized peptides were then tested in a screening assay for their comparative ability to serve as a substrate for DAPK. DAPK had a preference for peptides 1, 2, and 15 (Fig. 3A), which contain alanine, arginine, or threonine, respectively, at the P - 2 position (Table II). Peptides 1–18 were also tested for their ability to serve as substrates for MLCK. MLCK had a preference for alanine and threonine (data not shown) compared with DAPK, so arginine was held constant at this position in the synthesis of the library for the next (P - 1) position.

The second library of peptides synthesized had the sequence KKRQRXRSNVF, where *X* indicates the position at P - 1 that was varied among the peptides. The ability of peptides 19–35 to serve as substrates for DAPK is summarized in Fig. 3B. The screening results show that DAPK has a strong preference for leucine (peptide 27) and tyrosine (peptide 34) in the context of the KKRQRXRSNVF sequence. Therefore, subsequent libraries were made in parallel with either tyrosine or leucine held constant at P - 1.

Two libraries of peptides were made for the P1, one with the

P - 1 fixed as tyrosine (KKRPQRRYSXVF) and the other with the P - 1 fixed as leucine (KKRPQRRLSXVF). Activity analysis of the purified peptides from each library (peptides 36–69) revealed that DAPK has a clear preference for the amino acids asparagine and aspartic acid at the P1, regardless of whether P - 1 is tyrosine or leucine (Fig. 3, C and D). In contrast to the preferences of DAPK for this library, screening of peptides 36–69 with MLCK revealed a preference for glutamine and methionine at the P1 (data not shown), suggestive of increasing selectivity along with enhanced ability to serve as a DAPK substrate. Based on the available data at this point, peptides 38 and 55 were characterized further in order to determine if the goal of finding a peptide substrate for DAPK with a K_m value approaching $10 \mu\text{M}$ had been obtained yet.

As summarized below, peptides 38 and 55 have K_m values within the desired range. While the remaining investigations of DAPK enzyme activity utilized variations of these substrates, the profile of activity with the substrates from the different libraries suggested an emerging pattern for DAPK substrate preferences. In the core phosphorylation site, the emerging pattern is R(ART)(LYPMF)S(ND), where the parentheses indicate any of the included amino acids are potentially acceptable to DAPK. The selection of alanine at P - 2 combined with tyrosine or leucine at P - 1 clearly contributed a significant increase in utilization by DAPK with some enhancement of selectivity.

DAPK Catalytic Activity—Peptide 38 (KKRPQRRYSNVF) and peptide 55 (KKRPQRRLSNVF) were used in order to obtain the first kinetic values for a DAPK family member. Peptide 38 and peptide 55 are similar, with K_m values for DAPK of ~ 9 (Fig. 4) and $14 \mu\text{M}$, respectively. The kinetic data for DAPK

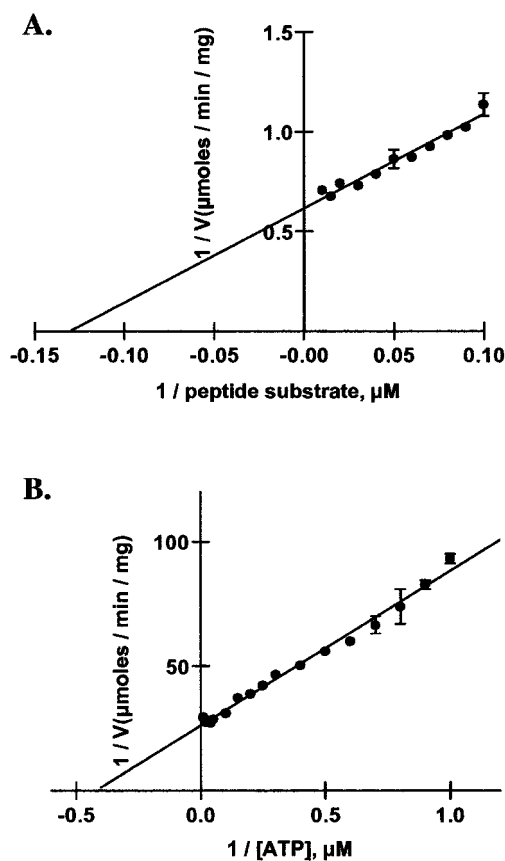


FIG. 4. **Kinetic analysis of DAPK.** A, double-reciprocal plot of the rate of peptide substrate phosphorylation as a function of peptide substrate concentration. The substrate concentration was varied from 10 to 100 μM . B, double-reciprocal plot of the rate of peptide substrate phosphorylation as a function of ATP concentration. The ATP concentration was varied from 1 to 50 μM . Peptide 38 was used as the substrate in all experiments. Data shown for each graph are from one representative experiment. Error bars indicate the standard errors from triplicate determinations and are not shown if the error is smaller than the symbol.

with ATP ($K_m = 2.4 \mu\text{M}$) using peptide 38 as the substrate are also shown in Fig. 4. The K_m values for peptides 38 and 55 represent a greater than 10-fold enhancement compared with the starting peptide 1 and attain the goal of discovering initial peptide substrates with K_m values of $\sim 10 \mu\text{M}$.

Once usable peptide substrates for DAPK were obtained, it was possible to address phosphate acceptor side chains at P0, which was raised by the analysis of the DAPK structure and peptide homology model. Specifically, the potential for threonine to be a phosphorylation residue instead of serine and the apparent rejection of tyrosine in this position were addressed. Peptide 70 (KKRPQRRYTNVF), in which a threonine replaced the serine, had a K_m value of 13 μM , consistent with threonine being an allowed phosphate acceptor. In contrast, peptide 71 (KKRPQRRYYNVF), in which a tyrosine replaced the serine, did not incorporate phosphate under the conditions of the assay, consistent with the lack of room in the active site of the structure to accommodate this bulkier side chain. With the recognition that DAPK could accommodate either a serine or a threonine as a phosphate acceptor side chain, we focused the subsequent investigations on DAPK enzyme activity in vertebrate tissue with the use of peptide 38.

DAPK mRNA is abundant in adult vertebrate brain (11). Therefore, brain tissue was used as a source of DAPK for initial investigations to demonstrate the potential biological utility of the discovered peptide substrates and to obtain the first infor-

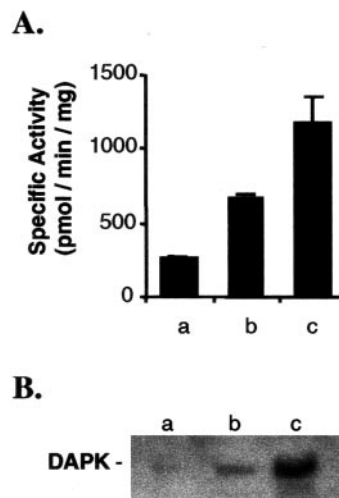
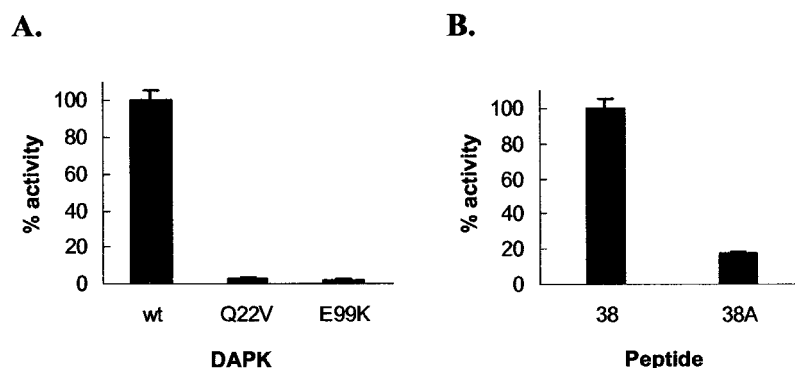


FIG. 5. **DAPK catalytic activity from vertebrate brain.** A, the increase in specific activity of brain DAPK with purification steps based on the properties of human DAPK predicted from the ORF of the cDNA is shown. B, the co-purification of the immunoreactive DAPK protein as determined by Western blot analysis with a site-directed antisera against the catalytic domain. The assay for DAPK activity is that developed as part of the substrate discovery reported here using peptide 38. The stages of DAPK purification are as follows: a, homogenate supernatant; b, ammonium sulfate precipitation fraction; and c, DEAE-chromatography purification step. Details of the purification steps are described in the text. For Western blot analysis, equal amounts of protein (30 μg) were taken for SDS-PAGE.

mation about the properties of DAPK enzyme activity in a vertebrate tissue. Specifically, the goals were to determine the feasibility of using peptide 38 and related peptides in assays of DAPK activity in tissue extracts, to verify that the enzyme activity measured in such an assay of a tissue extract copurifies with the kinase domain ORF, and to compare the enzymatic features of the tissue enzyme to the engineered catalytic domain produced in *E. coli*. We made an antisera targeted to the kinase domain in order to monitor by Western blot analysis the presence of the ORF-encoded kinase domain in a protein independent of activity measurements (see "Experimental Procedures"). We also developed a purification scheme for DAPK based on the predicted properties of the ORF encoded by the DAPK cDNA. These properties included a polypeptide chain mass of $\sim 160,000$ Da and a negative charge at neutral pH. If these were the properties of DAPK in adult brain, then both DAPK protein and DAPK enzyme activity should be recovered in parallel. Furthermore, if DAPK exists as a molecular complex that retains the features of the predicted ORF, then it should be recoverable and enhanced in specific activity using a standard protein chemistry protocol based on the predicted properties, such as adsorption to DEAE-cellulose at low ionic strengths and elution with low salt concentrations.

As summarized in Fig. 5, the enzyme activity measured by peptide 38 phosphorylation co-purified with the catalytic domain amino acid sequence as monitored by Western blot analysis. Briefly, fresh frozen bovine brain tissue was homogenized, and a soluble supernatant fraction was obtained by differential centrifugation. The supernatant was further fractionated by a 55% saturated ammonium sulfate precipitation step, and the ammonium sulfate precipitate containing DAPK was resuspended and then subjected to adsorption and step elution on a DEAE-cellulose ion exchange chromatography column. DAPK kinase activity and immunoreactive DAPK protein co-purified through the ammonium sulfate and DEAE cellulose chromatography fractionation (Fig. 5). The Western blot data shown in Fig. 5 were obtained with a site-directed antisera against the kinase domain (see "Experimental Procedures"). The same

FIG. 6. Probing potential key interactions by mutagenesis of DAPK and modification of peptide substrate. *A*, relative activity between wild type recombinant DAPK (*wt*) and DAPK mutants Q22V and E99K. The purified mutants were tested for activity using peptide 38 as a substrate under assay conditions identical to those used to measure the activity of wild type recombinant DAPK. *B*, relative phosphorylation of purified peptides 38 and 38A (AARPQRRYSNVF) by wild type recombinant DAPK. Assay conditions were the same as those used in the activity screening of the peptide substrate libraries. Data represent the average \pm the range of values for triplicates.



bands were detected with a commercially available antiserum made against the full-length protein that does not react with the kinase domain (data not shown). These results provide formal evidence that the DAPK ORF encoded by abundant mRNA is made as an endogenous protein in a vertebrate tissue and that vertebrate tissue DAPK has the properties predicted from analysis of the catalytic domain presented above.

The availability of a peptide substrate that could be used for quantitative analysis of DAPK enzyme activity in biological extracts made examination of endogenous catalytic activity possible. For example, kinetic analysis of brain DAPK, using peptide 38 as a substrate, revealed a K_m value of 10 μM . This is concordant with the K_m value of 9 μM for the DAPK catalytic domain produced in *E. coli*, an organism that lacks most of the post-translational modification machinery of eukaryotic cells. Furthermore, DAPK from vertebrate tissue (Fig. 5) has a specific activity similar to that of the catalytic domain produced in *E. coli*, indicative of DAPK from an adult tissue with comparatively high levels of the protein having a robust enzyme activity. Because a recent report (27) suggested that autophosphorylation might be a mechanism by which a DAPK-related protein keeps its kinase activity in a suppressed state until activated by cellular damage, we first addressed the potential for autophosphorylation of DAPK. We used CaMKII, the prototype for CaM-regulated autophosphorylation, as a positive control. Whereas CaMKII was autophosphorylated under the conditions used (see "Experimental Procedures"), there was no evidence of phosphate incorporation into adult brain DAPK protein, either in the presence or in the absence of Ca^{2+} /CaM (data not shown). Furthermore, the quantitative enzyme activity analyses of brain DAPK discussed above provided no indication of autophosphorylation effects on catalysis. Therefore, the similarity in enzyme activity between vertebrate tissue DAPK and the DAPK catalytic domain produced in *E. coli* and the failure to detect autophosphorylation with the vertebrate tissue enzyme raise the possibility that the pro-apoptotic role of DAPK is kept in check by mechanisms that remain to be characterized. Clearly, the regulation is more complex than previously assumed based on the presence of comparatively high levels and robust catalytic activity of DAPK in the healthy adult brain, an organ that should not be undergoing large scale apoptosis. Regardless, the results presented here validate the utility of peptide 38 and related substrates as a starting point for biological investigations.

DAPK Structure and Substrate Phosphorylation Site Recognition—The availability of a set of DAPK peptide substrates allowed further probing of the structure-assisted model for DAPK substrate recognition and catalysis. As noted above, there are certain amino acids in DAPK that are conserved throughout all serine/threonine PKs and should be addressed as a control experiment. For example, the glutamic acid that corresponds to Glu-99 of DAPK (see Fig. 1) is highly conserved

in all the kinases that have the phosphorylation motif RXXSX in their substrates, and mutagenesis of this position results in loss of activity among these serine/threonine protein kinases (14). The model for DAPK suggests that the arginine at the P - 3 of the RXXSX motif interacts with key residues in DAPK, such as Glu-99. Therefore, we mutated Glu-99 of DAPK to lysine in order to test correspondence between structure and activity. The mutant E99K-DAPK was purified and tested for its ability to phosphorylate peptide substrate 38. When tested for activity under identical conditions to unmodified DAPK (Fig. 3), the mutant E99K-DAPK had less than one-tenth the activity of the wild type enzyme in the screening assay (Fig. 6A).

Although less conserved across all serine/threonine PKs than Glu-99, Gln-22 is interesting as an additional test of the relation between the structure and substrate preference properties of DAPK. For example, Gln-22 of DAPK is in close proximity to peptide substrate positions P - 1, P0, and P1 (see Table I) and might be expected to play a key role in substrate recognition or catalysis. Because the corresponding amino acid in phosphorylase kinase is Val-29, we made a Q22V-DAPK mutant protein, and we examined the purified mutant DAPK activity with peptide 38 as a substrate. Again, this resulted in a loss of DAPK activity (Fig. 6A). This level of activity with peptide 38 and the mutant DAPKs is worse than that found with wild type DAPK and the starting peptide 1, consistent with a key role in activity for the potential complementary interactions between Gln-22 of DAPK and the core YSN and LSN sequences of the phosphorylation site in DAPK substrates.

As discussed previously, close inspection of the DAPK structure reveals a series of acidic amino acids and amino acid clusters that could complement potential basic amino acids of the substrate sequence in the area of P - 8 through P - 6. In order to assess the potential contribution of these amino-terminal basic residues upstream of the core phosphorylation site, we made and tested a variation of peptide 38, peptide 38A (AARPQRRYSNVF). Peptide 38A has the two amino-terminal lysine residues at P - 7 and P - 8 changed to alanines, thereby removing the side chain charge but retaining the peptide substrate length. When compared with peptide 38 in the screening assay, peptide 38A had less than half of the activity of peptide 38 (Fig. 6B). This demonstrates that, in the context of an efficient phosphorylation site amino acid sequence, a basic amino acid cluster upstream of the core phosphorylation site, in the approximate position of P - 6 to P - 8 in the substrate sequence, contributes to the substrate preferences of DAPK.

The results demonstrate the functional importance of broadly conserved and unique amino acids of DAPK that are in close proximity to the potential peptide substrate phosphorylation site sequences. Their importance in enzyme activity can be anticipated based on the structure of DAPK and the docked peptide substrate model. However, there is a novel feature of

the DAPK structure discovered during these investigations that is not addressed by the docked substrate model. This novel feature is the basic loop structure of DAPK that is composed of a cluster of arginine and lysine residues found in a short stretch of the amino acid sequence (indicated in Fig. 1). A similar cluster is found in the corresponding amino acid sequence region in other death kinases. Although the novel basic loop structure found in DAPK is near the peptide substrate recognition region, it is not as close in three-dimensional space to peptide substrate residues as the amino acids listed in Table I and addressed above. This means that the current model cannot anticipate the potential importance of this basic loop in substrate recognition. Therefore, the potential importance of this structure in substrate recognition was tested by site-directed mutagenesis of DAPK. Specifically, we made, purified, and tested for activity two double mutations of DAPK, R47A,R48A-DAPK and R53A,R54A-DAPK. However, these mutations did not have a significant effect on the K_m value of DAPK with peptide 38 as a substrate (*e.g.* the K_m is $\sim 13 \mu\text{M}$ for the R47A,R48A-DAPK). The site-directed mutagenesis results do not implicate the novel basic loop structure in the more intimate role of substrate recognition, such as that seen with DAPK amino acids in closer proximity. Conversely, the results do not address a potential effect on rate-limiting steps in the catalytic mechanism, such as release of phosphorylated product.

DISCUSSION

DAPK's discovery through a functional genetics screen (1) and the linkage of changes in DAPK levels to disease and injury (5–11) have made knowledge about this large multidomain protein critical to the advancement of several areas of biomedical research. The results summarized here fill a void in knowledge needed for further biological and clinical investigations of DAPK and related enzymes, and allow the refinement of prevailing hypotheses. The knowledge about DAPK activity, structure, and substrate recognition provides a firm foundation for current proteomics investigations that seek to determine which DAPK-binding proteins are potential kinase substrates. These tools and the knowledge emanating from this investigation should also enhance current searches for DAPK inhibitors. The insights into the protein kinase catalytic properties of adult brain DAPK raise interesting questions about the role of DAPK activity in neuronal homeostasis, differentiation, and cell death and indicate the need for a focused analysis of DAPK enzyme activity regulation. Finally, the discovery of the first peptide substrates for this orphan enzyme and the establishment of an activity assay provide a proof of principle for an experimental approach that can be potentially extended to other protein kinases without known substrates but identified through complete genome sequence analysis or functional genetics screens.

The activity data from mutagenesis of DAPK in the peptide substrate recognition region and from variation of the peptide substrate sequence can be integrated with the high resolution structure of the DAPK catalytic domain into a working model for DAPK substrate preferences. DAPK has a preference for sets of amino acid sequences in the core P -2, P -1, and P1, although a variety of amino acids are allowed at these positions, and DAPK has a loosely defined preference for basic amino acids in the substrate sequence that are further upstream around the relative position of P -7 and P -8. The emerging themes for DAPK substrate preference will allow prioritization of results from proteomics and genetics research targeted toward identification of endogenous DAPK substrates. For example, results from yeast two-hybrid screens with DAPK as a bait would be expected to identify a number of interacting

proteins based on the multiple association domains found in the DAPK amino acid sequence. However, those with the allowed pattern of amino acids in a potential phosphorylation sequence could be given priority as candidates for endogenous protein kinase substrates. The potential difficulty of this remaining task in protein substrate discovery can be appreciated by inspection of the literature for other protein kinases associated with cell death, such as receptor-interacting protein kinase (28), which have been placed into potential pathways based on their protein association domains but resisted integration into cellular pathways based on their kinase domain catalytic activity until recently (29).

The initial results on DAPK catalytic activity in vertebrate brain tissue raise a number of interesting questions, including an apparent paradox based on current knowledge. For example, DAPK mRNA is comparatively abundant in adult brain and increases in response to ischemia (11), which is characterized by post-stress neuronal apoptosis. Although the increase in DAPK mRNA in response to brain ischemia is consistent with its role as a proapoptotic kinase, the abundance of DAPK in adult brain prior to such injury raises the question of what role the DAPK catalytic activity is playing in the normal adult brain. One could speculate that the DAPK present in normal adult brain is well regulated through an autoinhibition mechanism, a redundant theme among CaM-regulated kinases (14). However, these mechanisms allow for transient activation through a release of autoinhibition in response to calcium signaling through CaM. The recent report (27) that DRP-1, a DAPK-like kinase, is held in check by a novel autophosphorylation mechanism is the foundation of the hypothesis that autophosphorylation of DAPK might act as an off switch to keep DAPK enzyme activity suppressed in normal adult brain. This hypothesis is especially interesting because the proposed autophosphorylation mechanism is an inactivating event, whereas all other regulations of CaMKs by autophosphorylation are activating events in terms of catalytic activity (14). Regardless, our straightforward tests of this hypothesis for DAPK regulation, using standard conditions for autophosphorylation and positive controls, did not reveal such a mechanism for brain DAPK. Furthermore, the brain DAPK has an enzyme activity profile similar to that of the isolated catalytic domain, and the brain DAPK enzyme activity co-purifies with the immunoreactive kinase domain during purification based on the predicted physical and chemical properties of the ORF. The results demonstrate that brain DAPK has a robust catalytic activity similar to that found in the isolated catalytic domain. Other assay conditions and tissue pretreatment might allow the detection of such a novel inhibitory autophosphorylation reaction and should be examined in future experiments. Alternatively, the array of other proteins and pathways present in normal adult brain may not be conducive to apoptosis and may reflect an entirely different function of DAPK. In this regard, DAPK discovery research may reveal alternative roles not directly related to its proapoptotic function, as was the case with the discovery (30) of alternative roles in brain for cyclin-dependent kinases not directly related to their role in cell cycle progression. Overall, the results reported here indicate the importance of further examination of the enzymology and mechanisms of action within the DAPK family of important serine/threonine PKs in order to fully integrate them into prevailing models of cellular regulation.

The straightforward and efficient approach that combines enzymology, structural biology, and parallel synthesis of substrate libraries should be readily applicable to protein kinase ORFs newly discovered as part of the genome sequence projects or functional genetic screens. It may be especially useful for

enzymes with more restricted substrate recognition characteristics, such as members of the DAPK and MLCK family. Such kinases cannot be assayed with the commonly used *in vitro* substrate peptides or proteins and appear not to have sufficient activity with the standard mixed peptide substrate libraries, which are expensive to screen and not commercially available. Furthermore, most current approaches for the study of peptide substrates (31) are geared toward optimization of the peptide substrate sequence after the discovery of the initial substrate, and newer approaches for discovery of novel protein substrates have started with a known efficient substrate as a foundation (32). Complementary to these other approaches, synthesis of positional scanning substrate libraries can allow rapid discovery of initial peptide substrates with the required kinetic properties, as shown here for protein kinases and elsewhere (26) for proteases. Once an initial substrate has been discovered and validated for biological use, such as that shown here for peptide 38, numerous alternative approaches are available for refinement and extension.

In addition to complementing other approaches, the knowledge base generated may also suggest new searches for potential physiological substrates based on informatics. For example, two proteins in the sequence data bases that have potential DAPK phosphorylation sites and have a known link to cell death are mouse p19ARF and Ca²⁺/calmodulin-dependent protein kinase kinase (CaMKK). It is not known if either of these proteins are effective protein substrates for DAPK, but reports in the literature make them and other proteins logical targets of ongoing investigations. For example, a comment in the Discussion of a recent paper (5) concerned with DAPK involvement in apoptosis and tumor suppression states that mouse p19ARF can be phosphorylated by DAPK *in vitro*. This is an attractive hypothesis because the authors (5) show in the body of the paper that DAPK is involved in the regulation of p19ARF and the resultant stabilization of p53. Another protein whose amino acid sequence also contains a potential DAPK phosphorylation site is CaMKK. CaMKK and the associated CaMK pathway has been suggested (33) as key to neuronal survival. Furthermore, a potential DAPK phosphorylation site is found near the carboxyl terminus of the proposed CaM recognition domain of CaMKK. Previous work with MLCK (34), as standard of comparison for CaM-regulated protein kinases (14), has linked phosphorylation sites in CaM recognition domains to down-regulation of CaM kinase activity. If relevant, the potential DAPK phosphorylation site in CaMKK could result in reduction of the proposed neuronal survival function of the CaMK pathway (33). These two examples of informatics-based hypothesis generation provide a potential p53-dependent and a potential p53-independent pathway to be examined in future research. Clearly, the presence of the motif in the sequence does not mean that the protein will be a substrate *in vitro* or *in vivo*. However, these examples serve to demonstrate yet another potential biological application of the body of knowledge resulting from the experimental approach. Regardless of the ultimate outcome of studies on these two examples, the availability of active DAPK protein preparations, a DAPK activity assay, a family of peptide substrates validated for biological studies, and a high resolution structure should facilitate the

continued investigation of DAPK biology as well as the discovery of small molecule, cell-permeable modulators of DAPK function as drug discovery leads.

Acknowledgments—We thank T. Lukas, S. Mirzoeva, and J. Schavocky for their generous assistance and advice and Dr. Linda Van Eldik for constructive criticism during the course of the investigations.

REFERENCES

- Deiss, L. P., Feinstein, E., Berissi, H., Cohen, O., and Kimchi, A. (1995) *Genes Dev.* **9**, 15–30
- Raveh, T., Berissi, H., Eisenstein, M., Spivak, T., and Kimchi, A. (2000) *Proc. Natl. Acad. Sci. U. S. A.* **97**, 1572–1577
- Cohen, O., Inbal, B., Kissil, J. L., Raveh, T., Berissi, H., Spivak-Kroizaman, T., Feinstein, E., and Kimchi, A. (1999) *J. Cell Biol.* **146**, 141–148
- Inbal, B., Shani, G., Cohen, O., Kissil, J. L., and Kimchi, A. (2000) *Mol. Cell Biol.* **20**, 1044–1054
- Raveh, T., Drogue, G., Horwitz, M. S., DePinho, R. A., and Kimchi, A. (2001) *Nature Cell Biol.* **3**, 1–7
- Esteller, M. (2000) *Eur. J. Cancer* **36**, 2294–2300
- Katzenellenbogen, R. A., Baylin, S. B., and Herman, J. G. (1999) *Blood* **93**, 4347–4353
- Nakatsuka, S., Takakuwa, T., Tomita, Y., Miwa, H., Matsuzuka, F., and Aozasa, K. (2000) *Lab. Invest.* **80**, 1651–1655
- Tang, X., Khuri, F. R., Lee, J. J., Kemp, D. L., Hong, W. K., and Mao, L. (2000) *J. Natl. Cancer Inst.* **92**, 1511–1516
- Sanchez-Cespedes, M., Esteller, M., Wu, L., Homaira, N., Yoo, G. H., Koch, W. M., Jen, J., Herman, J. G., and Sidransky, D. (2000) *Cancer Res.* **60**, 892–895
- Yamamoto, M., Takahashi, H., Nakamura, T., Hioki, T., Nagayama, S., Oashi, N., Sun, X., Ishii, T., Kudo, Y., Nakajima-Iijima, S., Kimchi, A., and Uchino, S. (1999) *J. Neurosci. Res.* **58**, 674–683
- Lander, E. S., et al. (2001) *Nature* **409**, 860–921
- Cohen, O., Feinstein, E., and Kimchi, A. (1997) *EMBO J.* **16**, 998–1008
- Lukas, T. J., Mirzoeva, S., and Watterson, D. M. (1998) in *Calmodulin and Signal Transduction* (Van Eldik, L., and Watterson, D. M., eds) pp. 65–168, Academic Press, New York
- Watterson, D. M., Schavocky, J. P., Guo, L., Weiss, C., Chlenski, A., Shirinsky, V. P., Van Eldik, L. J., and Haiech, J. (1999) *J. Cell. Biochem.* **75**, 481–491
- Shoemaker, M. O., Lau, W., Shattuck, R. L., Kwiatkowski, A. P., Matrisian, P. E., Guerra-Santos, L., Wilson, E., Lukas, T. J., Van Eldik, L. J., and Watterson, D. M. (1990) *J. Cell Biol.* **111**, 1107–1125
- Watterson, D. M., Collinge, M., Lukas, T. J., Van Eldik, L. J., Birukov, K. G., Stepanova, O. V., and Shirinsky, V. P. (1995) *FEBS Lett.* **373**, 217–220
- Van Eldik, L. J., Fok, K. F., Erickson, B. W., and Watterson, D. M. (1983) *Proc. Natl. Acad. Sci. U. S. A.* **22**, 6775–6779
- Zhou, Z. H., Ando, S., Furutsuka, D., and Ikebe, M. (1995) *Biochem. J.* **310**, 517–525
- Lukas, T. J., Mirzoeva, S., Slomczynska, U., and Watterson, D. M. (1999) *J. Med. Chem.* **42**, 910–919
- Lowe, E. D., Noble, M. E., Skamnaki, V. T., Oikonomakos, N. G., Owen, D. J., and Johnson, L. N. (1997) *EMBO J.* **16**, 6646–6658
- Kogel, D., Plottner, O., Landsberg, G., Christian, S., and Scheidtmann, K. H. (1998) *Oncogene* **17**, 2645–2654
- Kawai, T., Nomura, F., Hoshino, K., Copeland, N. G., Gilbert, D. J., Jenkins, N. A., and Akira, S. (1999) *Oncogene* **18**, 3471–3480
- Sanjo, H., Kawai, T., and Akira, S. (1998) *J. Biol. Chem.* **273**, 29066–29071
- Kawai, T., Matsumoto, M., Takeda, K., Sanjo, H., and Akira, S. (1998) *Mol. Cell Biol.* **18**, 1642–1651
- Backes, B. J., Harris, J. L., Leonetti, F., Craik, C. S., and Ellman, J. A. (2000) *Nat. Biotechnol.* **18**, 187–193
- Shani, G., Henis-Korenblit, S., Jona, G., Gileadi, O., Eisenstein, M., Ziv, T., Admon, A., and Kimchi, A. (2001) *EMBO J.* **20**, 1099–1113
- Stanger, B. Z., Leder, P., Lee, T., Kim, E., and Seed, B. (1995) *Cell* **81**, 513–523
- Kim, J. W., Joe, C. O., and Choi, E.-J. (2001) *J. Biol. Chem.* **276**, 27064–27070
- Padmanabhan, J., Park, D. S., Greene, L. A., and Shelanski, M. L. (1999) *J. Neurosci.* **19**, 8747–8756
- Songyang, Z., Lu, K. P., Kwon, Y. T., Tsai, L. H., Filhol, O., Cochet, C., Brickey, D. A., Soderling, T. R., Bartleson, C., Graves, D. J., DeMaggio, A. J., Hoekstra, M. F., Blenis, J., Hunter, T., and Cantley, L. C. (1996) *Mol. Cell Biol.* **16**, 6486–6493
- Habelhah, H., Shah, K., Huang, L., Burlingame, A. L., Shokat, K. M., and Ronai, Z. (2001) *J. Biol. Chem.* **276**, 18090–18095
- Yano, S., Tokumitsu, H., and Soderling, T. R. (1998) *Nature* **396**, 584–587
- Lukas, T. J., Burgess, W. H., Prendergast, F. G., Lau, W., and Watterson, D. M. (1986) *Biochemistry* **25**, 1458–1464